



AN EXPERIMENTAL AND NUMERICAL STUDY ON THE EFFECTS OF TAPER ANGLES AND OVERLAP LENGTH ON THE FAILURE AND STRESS DISTRIBUTION OF ADHESIVELY-BONDED SINGLE-LAP JOINTS

Murat Yavuz Solmaz and Aydın Turgut
Department of Mechanical Engineering, Faculty of Engineering
Firat University, 23119 Elazig, Turkey
mysolmaz@firat.edu.tr

Abstract – This paper examines the failures and strengths of joints bonded by a Neoxil CE92 N8 adhesive at different overlap lengths and different taper angles. The study was carried out both as experimental and numerical. In the experimental stage, lap-shear tests on Single-Lap Joints (SLJs) with different taper angles and overlap lengths were conducted. The stress analyses in the SLJs were obtained using a linear Finite Element Analysis (FEA) in numerical stage. It is assumed that adhesive and adherend have both geometrical nonlinearity and linear material behaviour. Scrutinising carefully the surfaces of the SLJs, two different failure types, cohesive failures (CF) and special cohesive failures (SCF) were observed. The obtained numerical results were compared with experimental ones. Results indicate that the increasing of both overlap length and taper angle increase the joint strength and, in particular, the highest strength values in all joint geometries are attained by specimens having a taper angle of 15° .

Key-Words- Adhesive, Taper Angle, Single Lap Joint, Finite Element Stress Analysis

1. INTRODUCTION

During the past two decades or so, important progress has been witnessed in composite materials and their production methods. Such a development has provided a new application area for the polymer matrix composite materials in many components of air vehicles [1]. In addition, the rapid progress has brought about influential and reliable improvements in the bounding methods of structural elements and the adhesively bonding methods that are alternative to the mechanical fastening due to the problems such as drilled holes, broken fibres, and stress concentrations [2].

The mechanical behaviour of the adhesively bonded joints depends on such parameters as the geometrical properties of the joints and on the properties of materials from which it is fabricated. This dependence complicates the prediction of the overall mechanical behaviour of the joint. In order to understand the mechanical behaviour of adhesively bonded joints, many studies have been carried out, different models have been proposed and different methods have been used. One of these methods is based on the strength of materials. This method assumes that failure occurs when the equivalent strain or stress calculated at any point of the adhesive layer or adherends reach the ultimate strain or stress of the materials [3], [4]. Hart-Smith [3] first examined the growth of plastic deformation regions in the elastic-plastic adhesive layer of different types of adhesive joints, and showed that the plastic deformation regions appeared at the free end of the adhesive layer. Wah analysed the stress distribution using the plane

strain assumption in a Single Lap Joint (SLJ) in which anisotropic material is adhesively bonded. He argued that the bending moments in the bonded materials display the highest values on the free ends of the joint [5]. Chang and Muki indicated that the geometry of the adherend at the ends of the adhesive line was very important in governing the normal and shear stresses which occur in the adhesive layer of adhesively bonded joints [6]. An experiment studying the effect of adhesive area on the joint strength in [7] showed that shear strength decreases considerably as the bonding area expands, which could be the result of the fact that deformation resistance occurring in small areas was more than those of large areas. Apalak and Güneş studied the thermal stress analysis of SLJs. Detailed analysis showed that the most critical bonding region is the free ends of the adhesive-adherend material interface; in addition, thermal loads led to serious strain and stress concentrations similar to those of structural loads [8]. Abedian and Szyszkowski examined theoretically the effects of surface geometry of the composite material on the thermal stress distribution and inferred that the stress state near free edges of the adherends was very sensitive to the geometrical properties of surface [9]. Sancaktar and Simmons examined both numerically and experimentally the effect of a notch generated on the bonded material and their deformation behaviour on the strength of the SLJs. Experimental results showed that the strengths of notched material were about 29% higher than those of the non-notch materials. Their Finite Element Analysis (FEA) predicted 27% decrease at the peak stress values [10]. Avila et al. studied the stress analysis of the wavy-lap joint in composites. Based on both experiments and FEA, they determined a 41% increase in the load capacity and found out that this increase was caused by compressive stresses areas which occur in the wavy-lap joints [11]. Lang and Mallick examined the effect of different spew shapes on the stress distribution and maximum stress by examining different spew geometries at a SLJs [12]. Using two-dimensional FEA, Özel et al. examined the elasto-plastic stress analysis of SLJs subject to a bending moment in SLJs with very different mechanic properties from each other consisting of the hardened steel bonded material and two adhesives, one of which was stiff and the other was flexible. They observed that the adhesive thickness had critical effect on the joint strength and argued that the load borne by the SLJ bonded by an adhesive with the capability of changing high shape increase with increasing overlap length [13]. Aydin et al. presented a new approach by using nonlinear FEA for determining the failure type and strength of a joint bonded by a film type of adhesive. First, they conducted the lap-shear test on SLJs with four different adherend thickness and overlap lengths and examined the fracture surfaces using scanning electron microscopy. Then they conducted the stress analyses on SLJs taking into consideration both the geometrical nonlinearity and nonlinear material behaviour of the adhesive and the adherends. They noted two different failure types at SLJs failure surfaces. One of them was caused by the peel stress with the tensile failures at the free ends of the adhesive layer; the other was the result of shear stress near the centre of overlap region [14].

This paper presents an approach using linear FEM to estimate the failure and strength of joints bonded by a stiff adhesive (Neoxil CE92 N8) with different overlap lengths and different taper angles. The approach had the following steps: First, lap-shear tests on Single-Lap Joints (SLJs) with different taper angles and overlap lengths were carried out and then stress analyses at the SLJs were performed by considering both the

geometrical non-linearity and linear material behaviours of adhesive and adherend by using the linear FEA; then, FEA results were compared with experimental results as the final step.

2. JOINT CONFIGURATIONS AND MATERIAL PROPERTIES

In this section, the properties of materials are introduced. Neoxil CE 92 N8 and Carbon Fiber Reinforcement Polymer (CFRP) were used as adhesive and adherends respectively in this study. The adherend surfaces cleaned with acetone were bonded as shown in Fig.1 under the pressure 0.155 MPa for 60 minutes. All specimens were cured at the constant room temperature set to 23 °C for 96 hours. The adherend thickness (t) used with all SLJs is 3.175 mm and their width (w) is 12.7 mm. On the other hand, the thickness of their adhesive layers (n) was separately measured at the finish of the experiments and their mean value was computed as 0.2 mm.

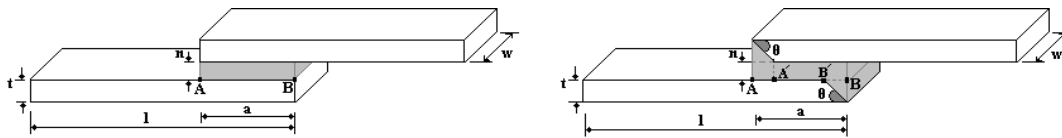


Figure 1 - Configuration of SLJs a) with no angle and b) with angles.

In this study, six different taper angles, θ and two different overlap lengths, a , were taken into consideration. These overlap lengths were 25.4 mm and 38.1 mm. First the case with no angle (0°) and then the cases with the taper angles of 15° , 30° , 45° , 60° , and 75° were constructed for each overlap length. The lap-shear tests were individually conducted for each case. In Table 1, the drawings of the specimens with no angle and with angles are presented.

The total bonding area is equal to the numerical multiplication of the overlap length, a , and the material width, w . This area increases when both the taper angle and the overlap length rise. In addition, the area increases if only taper angle is increased by keeping constant the overlap length. Therefore the bonding area generating at each angle value should have numerically identical sizes in order to be able to observe the effect of the taper angle. In order to reach the objective aimed at by this study, the overlap lengths to be satisfied were determined, the constant total bonding area was set to 384.461 mm^2 at each taper angle and finally experiments were conducted for the obtained overlap lengths. Thus, the effect of taper angle was examined as independent from the total bonding area. The taper angle, the overlap length, and the total bonding area used at the experimental and numerical studies are given in Table 1.

The mechanical properties of adhesive and adherend used in this study was determined by the results of the experiments realized by applying the strain experiment principles defined in ASTM E8 (1999) to bulk specimens of these materials. The stress-strain behaviours of adhesive and adherend are necessary for elastic stress analysis via linear FEM. The obtained stress-strain characteristics of adhesive and adherend are shown in Fig. 2 and the geometrical parameters and material properties of adhesive and adherend used in the FE analysis are given Tables 1, 2 and 3, respectively. More information on the mechanical behaviour of Neoxil CE92 N8 can be found in [15].

Table 1 SLJs parameters used at the experimental and numerical studies.

| Overlap length (a) | Taper angle (θ) | Total Bonding Area (mm^2) |
|--------------------|--------------------------|--------------------------------------|
| 25.4* | 0 | 322.580 |
| 25.4 | 15 | 333.197 |
| 25.4 | 30 | 344.188 |
| 25.4 | 45 | 355.984 |
| 25.4 | 60 | 369.140 |
| 25.4 | 75 | 384.461 |
| ----- | | |
| 38.1** | 0 | 483.870 |
| 38.1 | 15 | 494.487 |
| 38.1 | 30 | 505.478 |
| 38.1 | 45 | 517.274 |
| 38.1 | 60 | 530.430 |
| 38.1 | 75 | 545.751 |
| ----- | | |
| 30.27 | 0 | 384.461 |
| 29.43 | 15 | 384.461 |
| 28.57 | 30 | 384.461 |
| 27.64 | 45 | 384.461 |
| 26.60 | 60 | 384.461 |
| 25.40 | 75 | 384.461 |

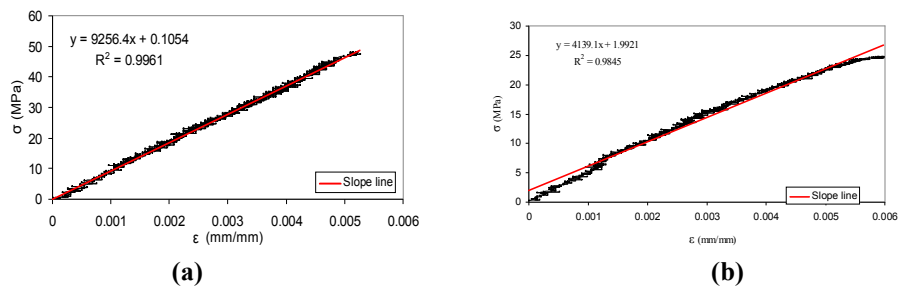
* 25.4 mm = 1", ** 38.1 mm = 1.5"

Table 2 - Material properties of the CFRP [15].

| | |
|---|-------|
| Longitudinal elastic modulus, E_1 (MPa) | 9284 |
| Transverse elastic modulus, E_2 (MPa) | 2816 |
| In-plane shear modulus, G_{12} (MPa) | 1862 |
| Major Poisson's ratio, ν_{12} | 0.31 |
| Ultimate strength, σ^* (MPa) | 48.04 |

Table 3 - Material properties of Neoxil CE92 N8 [15].

| | |
|-------------------------------------|------|
| Elastic modulus, E (MPa) | 4152 |
| Poisson's ratio, ν | 0.35 |
| Ultimate strength, σ^* (MPa) | 24.7 |

**Figure 2** - The tensile stress-strain behaviour of (a) CFRP adherend and (b) Neoxil CE92 N8 adhesive.

3. FINITE ELEMENT MODELLING OF SLJS

In this step, a three-dimensional finite element analysis was employed in order to analyze the behaviour of the SLJ with different taper angles and overlap lengths in Table 1. Analysis was performed using the ANSYS 10.0 software [16].

In the analysis, linear material behaviour based on the uni-axial stress-strain behaviours of adhesive (Neoxil CE92 N8) and adherend (CFRP) in Fig. 2 were examined. Moreover, the stress analysis of SLJs was obtained according to von Mises yield criterion. By means of this criterion, the equivalent stress (σ_{eq}) distribution in the adhesive layer and adherends were calculated.

A three-dimensional model of each CFRP adherend was generated using Solid 64 elements. The element is composed of eight different nodes with three degrees of freedom: translations in the nodal x, y, and z directions. On the other hand, 8-node solid element and Solid 45 were used for modelling the adhesive layer. The Solid 45 element consists of eight different nodes with three degrees of freedom: translations in the nodal x, y, and z directions.

The loading and boundary conditions considered in this study are presented in Fig.3. Tensile load is applied in the x direction [17].

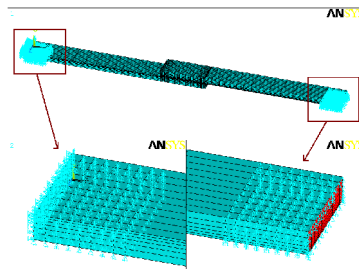


Figure - 3 Loading and boundary conditions of all models [17].

The mesh structure of the models generated in ANSYS is shown in Fig. 4. The most critical region from the point of view of stress is the region in which the bonding process is performed. The meshing in the critical region is performed in a more sensitive manner by dividing it into small pieces as shown in Fig. 4. In this study, since the effects of the overlap length and taper angle were examined, the element dimension and mesh density should not affect the analysis results. Hence the same element dimension was used in all models as often as practicable.

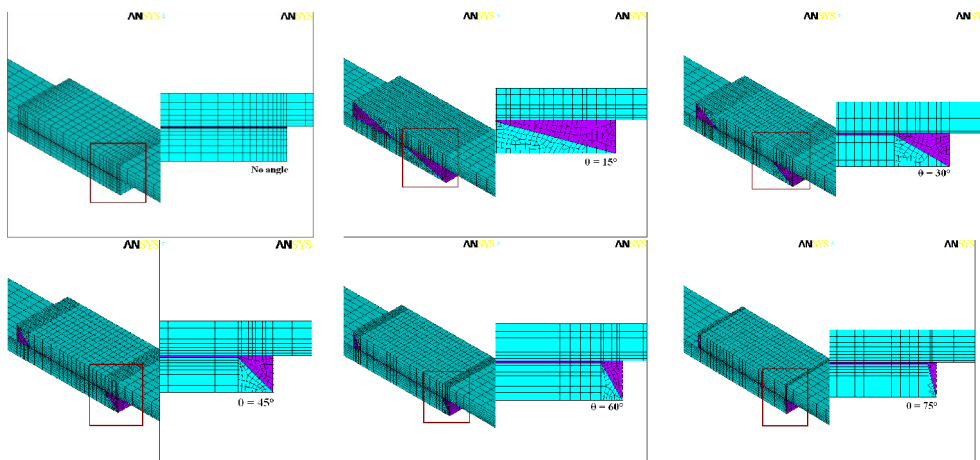


Figure - 4 Mesh views of the finite element models for the joint geometries at six different taper angles.

4. RESULTS AND DISCUSSION

4.1. Experimental Results

Experimental studies were carried out to test the accuracy and effectiveness of the proposed numerical analyses. The experiments were conducted at the crosshead speed of 1 mm/min by computer-controlled UTEST 15 (1kN) universal test equipment at 23 °C room temperature and 50% \pm 5 room humidity.

Because of being eccentric with the force applied to the specimens the adherends were exposed to bending moment reveals on the overlap region. The moment causes the peel stress by generating the rotations at the free ends of the overlap region. While the rotation angle grows, a crack appears and grows as well. Finally, the failure occurs instantly when the cross-section area the crack reaches a certain value [18]. In our specimens bonded with Neoxil CE92 N8, a small amount of peel effect occurred for each overlap length and the failure instantly took place without observing any initial failure.

Upon examining the failure in the overlap region of the specimens bonded with the taper angle 0°, it was observed that the failure was a cohesive failure (CF) and the quantity of the adhesive layer remaining on the surface of the bonding both materials was equal. On the other hand, a special cohesive failure (SCF) was observed in the specimens with the taper angles 15°, 30°, 45°, 60°, and 75° and it was determined that the quantity of the remains on one of bonded materials was more than that of the other. The obtained all results are displayed in Fig. 5.

The specimens were carefully and closely observed in order to understand the failure mechanism during the tensile tests. After the tests were finished, the specimen dimensions and the failure forces were recorded. As can be clearly seen from Fig. 6, the lowest failure force was determined at the taper angle 0° for each overlap length.

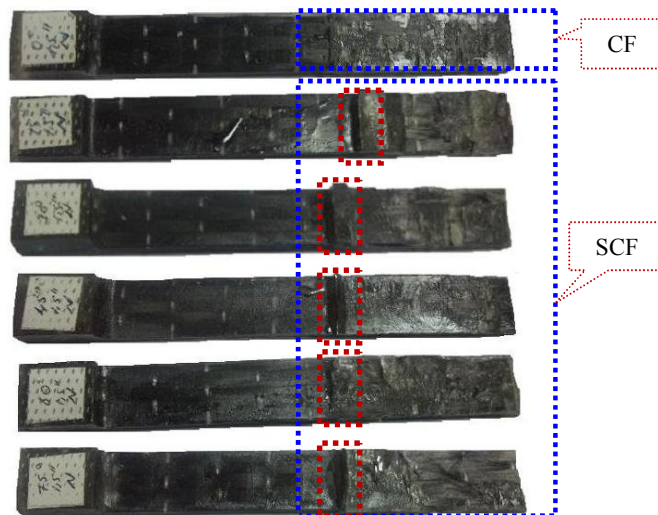


Figure - 5 The failure types in the overlap region of the specimens bonded with the 1.5 inches.

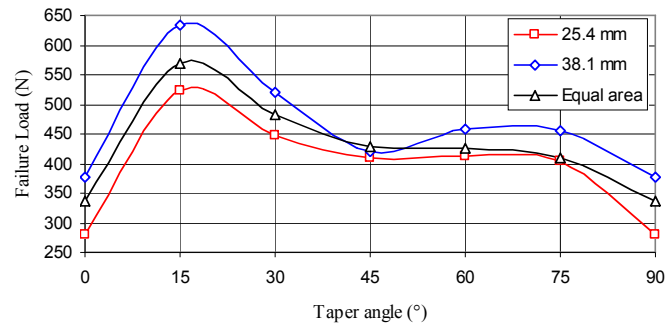


Figure - 6 Variation of experimental failure force with respect to the taper angles and the overlap lengths of SLJs bonded by Neoxil CE92 N8.

However, the highest failure force was found out at the taper angle 15° for each overlap length. One inference was that, after 15°, the failure force started to decrease but these forces were more than those of the ones determined at the taper angle 0° for each overlap length. In addition, the force generating failure also increased as the overlap length values increased for the same angle. For instance, a failure force of 279 N was obtained at the overlap length of 25.4 mm. When the overlap length was increased to 38.1 mm the failure force ascended to 376 N which represents some 1.35 times increase(376/279).

4.2. Finite Element Analysis Results

In this section, the effectiveness and accuracy of FEA is discussed by comparing it with that of the experimental results as $\sigma_{\text{Neoxil}} = 24.7 \text{ MPa}$. The ultimate stress was stated as σ^* on the demonstrated graphics.

When an adhesively bonded joint is loaded, a three dimensional stress appears. Equivalent stress, σ_{eq} , was computed using von Mises yield criterion. Moreover, it was accepted that the failure occurred when the equivalent stress reached to the ultimate stress of the adhesive at any point of the adhesive layer.

The critical region at the SLJs with different taper angles is the interface of bonded material with adhesive. Accordingly, the stress analysis in the adhesive layer was accomplished along the line A-B shown in Fig 1a and 1b. In order to compare the stress distributions generated at the adhesive layer, the stress on the adhesive layer throughout A-B line was normalized by dividing by the ultimate stress of the adhesive bulk specimen, σ_{Neoxil} . Similarly, the coordinate value on the horizontal axis of the setup. To estimate the failure load for the FEA, the ultimate stress of the adhesive was taken from experimental point for computing the stress distribution, x , was normalized by dividing by the overlap length, a , for comparing the stress distributions generating at different overlap lengths.

In addition, the numerical failure load of each specimen was determined by the multiplication of the stress values obtained using FEA by the area where the force was applied. Approximation correction was computed by the ratio of the experimental failure loads P_{FM} and the numerical failure loads P_{FM}^* . Consequently, it was observed that the experimental and numerical results in Table 4 coincided with each other, and that the approximation correction was close to 1.

Since the load carried by adherend causes the lateral tensile stresses by preventing shrinkage in free way, an adhesively-bonded joint expose to both the stresses of the transverse peeling (σ_y) and shear (τ_{xy}) and two normal tensions that are parallel and vertical to the joint. In other words, the deformation areas near the ends of the joint occur in three-dimensional [19], [20].

As a result of the finite elements analysis, the distribution of stress components obtained throughout the A-B line on the adhesive layer showed almost the same values for all three overlap lengths. Therefore, the graphics of stress distribution obtained from only the specimens with 25.4 mm overlap length are given in this paper.

Table 4 Experimental and estimated failure loads of the considered SLJs at different taper angles and overlap length.

| a (mm) | θ (°) | Area (mm ²) | P_{FM} (N) | P_{FM}^* (N) | P_{FM}/P_{FM}^* | Failure Type |
|--------|--------------|-------------------------|--------------|----------------|-------------------|--------------|
| 25.4 | 0 | 322.580 | 279.186 | 290.789 | 0.960 | CF |
| 25.4 | 15 | 333.197 | 522.695 | 506.434 | 1.032 | SCF |
| 25.4 | 30 | 344.188 | 447.931 | 414.483 | 1.080 | SCF |
| 25.4 | 45 | 355.984 | 408.579 | 386.660 | 1.056 | SCF |
| 25.4 | 60 | 369.140 | 411.937 | 386.802 | 1.064 | SCF |
| 25.4 | 75 | 384.461 | 404.529 | 368.753 | 1.097 | SCF |
| ----- | | | | | | |
| 38.1 | 0 | 483.870 | 376.606 | 344.588 | 1.092 | CF |
| 38.1 | 15 | 494.487 | 632.540 | 584.394 | 1.082 | SCF |
| 38.1 | 30 | 505.478 | 519.137 | 471.987 | 1.099 | SCF |
| 38.1 | 45 | 517.274 | 420.978 | 435.701 | 0.966 | SCF |
| 38.1 | 60 | 530.430 | 458.148 | 432.680 | 1.058 | SCF |
| 38.1 | 75 | 545.751 | 454.492 | 419.193 | 1.084 | SCF |
| ----- | | | | | | |
| 30.27 | 0 | 384.461 | 336.365 | 308.935 | 1.088 | CF |
| 29.43 | 15 | 384.461 | 570.261 | 526.076 | 1.083 | SCF |
| 28.57 | 30 | 384.461 | 481.132 | 430.644 | 1.012 | SCF |
| 27.64 | 45 | 384.461 | 427.557 | 391.230 | 1.092 | SCF |
| 26.60 | 60 | 384.461 | 425.154 | 390.354 | 1.089 | SCF |
| 25.40 | 75 | 384.461 | 408.129 | 368.753 | 1.011 | SCF |

In Fig. 7, as a result of the finite elements analysis, normal (σ_x , σ_y and σ_z), shear (τ_{xy}) and equivalent (σ_{eq}) stress distributions obtained from the adhesive layer throughout A-B line at 25.4 mm overlap length have been given. A general examination of this figure disclosed that maximum values of all stress components located at the end sections at $x/a = 0$ and $x/a = 1$ meaning the end sections of the overlap area.

Thanks to Fig. 7a, it was observed that maximum and minimum values of normal stress σ_x occurred at 0° and at 15°, respectively. As the taper angle was increased, the stress values increased also. On the other hand, in interval $0.1 \leq x/a \leq 0.9$, it was obtained higher values with respect to other angle values at 15° in contrary to the situation at the end sections.

Maximum value of normalized peeling stresses (σ_y/σ^*) determined as 1.1173 at 0° by means of Fig. 7b. This value is almost 2.153 times higher than the value 0.5189 at 75° which yields the closest result to it. Taper angle did not have any effect on the peeling stress in interval $0.2 \leq x/a \leq 0.8$ of overlap area.

Taking into consideration Fig. 7c, it was determined that σ_z stress distribution was almost the same characteristics with σ_y distribution and stress values were obtained as almost half of the σ_y stress values.

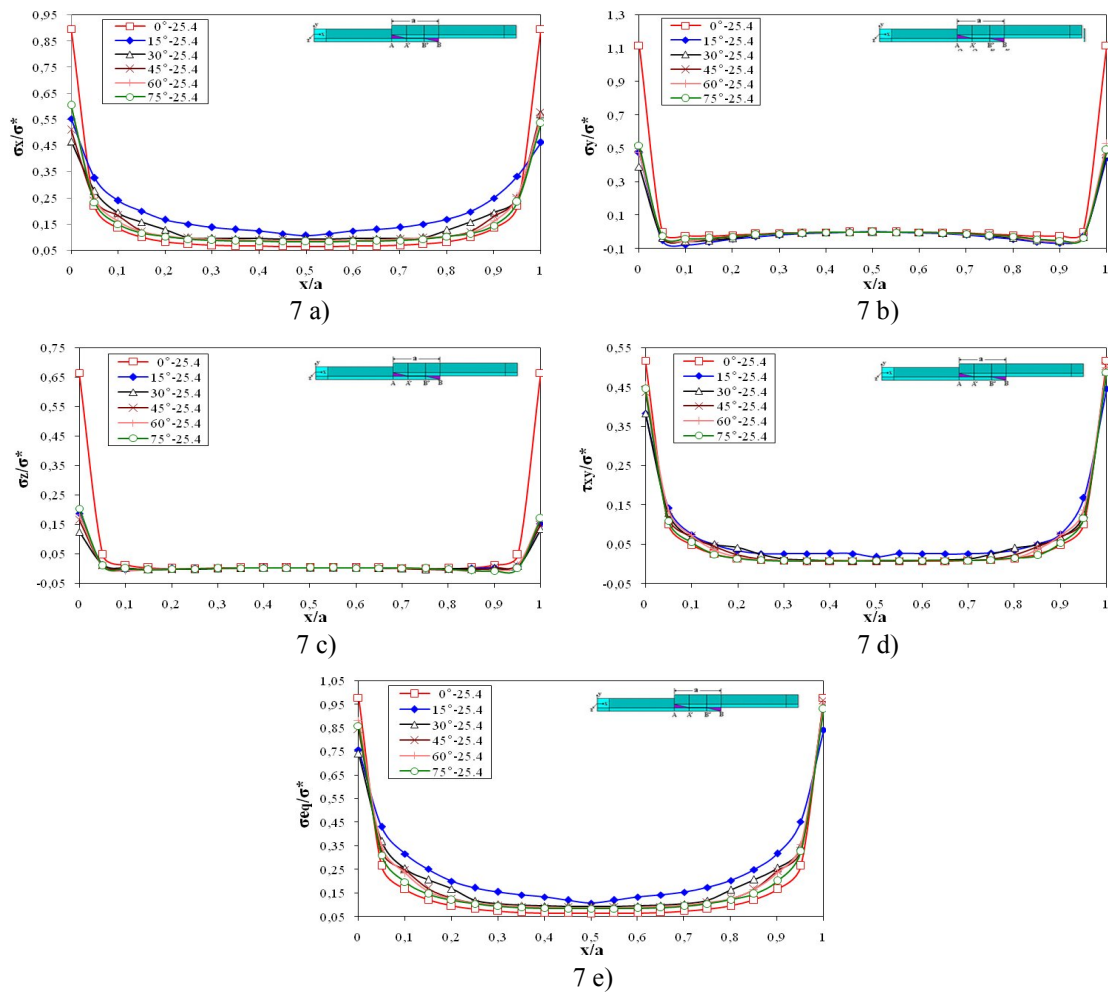


Figure - 7 Stress distributions obtained from the adhesive layer throughout A-B line at 25.4 mm overlap length: a) normalized σ_x stress distributions; b) normalized transverse peeling stress (σ_y) distributions; c) normalized σ_z stress distributions; d) normalized shear stress (τ_{xy}) distributions and e) normalized equivalent stress (σ_{eq}) stress distributions.

Figs. 7d-e exhibited that in similar way that of normal stress components, the maximum and minimum values of shear (τ_{xy}) and equivalent stress (σ_{eq}) distributions were respectively at taper angles 0° and 15° at the end sections of the overlap area at the bonded specimens.

The stress distribution characteristic in the overlap area is almost identical for the 3 overlap lengths, therefore, instead of graphics showing the stress distributions,

maximum values of the stress components that occur in along A-B line depending on the taper angle changes are given in Fig. 8 for the specimens with equivalent-area and the overlap lengths of 25.4 mm, 38.1 mm.

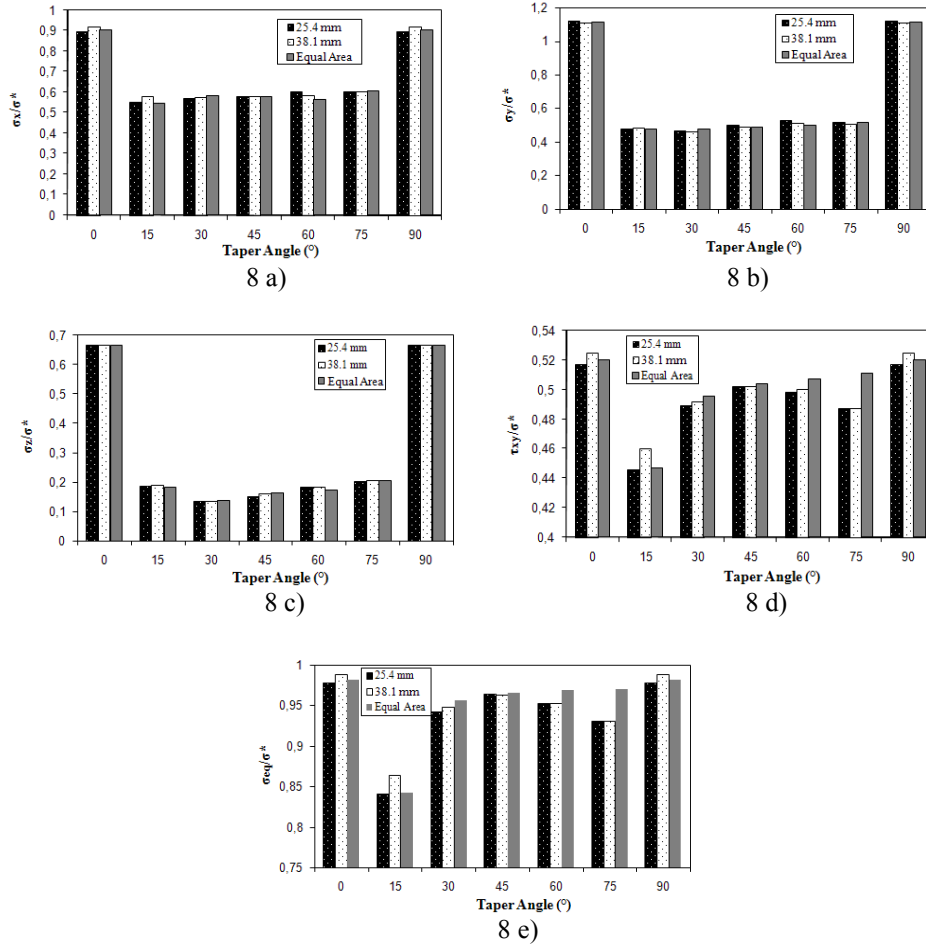


Figure - 8 Maximum values of stress components for all overlap lengths and taper angles a) normal σ_x , b) transverse peeling σ_y , c) normal σ_z , d) shear τ_{xy} and e) equivalent (σ_{eq}) stress

Examining Figs. 8a,b,c, it was determined that maximum values for normal (σ_x), transverse peeling (σ_y) and normal (σ_z) stress components occurred at taper angle 0° for all overlap lengths at the bonded joints, and however that maximum stress values occurring at intermediary angle values were different for different components but they were close to each other.

On the other hand, Figs. 8d-e indicated that maximum and minimum values for shear (τ_{xy}) and equivalent stress (σ_{eq}) distributions revealed at taper angles 0° and 15° respectively at the bonded specimens.

5. CONCLUSION

Accurately identified mechanical characteristics of structural adhesives are needed in order to determine the failure criterions during the design of adhesive joint and calculate the stress distributions at loaded joints.

In this paper, adherends with different taper angles at different overlap lengths were joined using Neoxil CE92 N8. By subjecting to tensile test obtained specimens, failure strengths and failure types of joints were identified.

As a result of the tensile test, following findings were obtained:

When the adhesion surfaces with failure were examined for all overlap lengths and all angle values, it was observed that type of failure occurring in specimens with taper angle of 0° (90° or no angle) was “cohesive failure” and those of specimens with the other angle values were “special cohesive failure”.

Strength of joints is at its lowest value at 0° generally. When taper angle is increased, cohesive strength also increases. When the taper angles used in the study were examined, maximum strength observed at joints with 15° taper angle.

Comparing the failure loads estimated by the analysis of finite elements to the failure loads obtained by tensile test, it was seen that they were in rather harmony to each other.

Results of finite element analysis depicted that maximum equivalent stresses occurring at adhesively bonded joints subject to tensile load took place at the interface between adhesive and adherend.

The most critical points were appeared at $x = 0$ and $x = a$ (the points A and B) for all specimens joined at 0° . Increasing overlap length, the amount of load that can be carried by the joint increased in particular at the specimens bonded at 0° (90° or no angle).

Experimental and numerical studies conducted in order to observe only the effect of taper angle showed that maximum stress occurred at the end sections of the joint and 0° , whereas minimum stress occurred at 15° .

When the peeling stresses in the joints bonded with the angle values in the interval 0 and 15° were scrutinized, it was observed that the difference between maximum value and minimum value them was almost 2.35 times of minimum one. This result showed that free taper angle should be the central focus of attention at the adhesively-bond joint designs.

In this study, the most suitable taper angle value for increasing the performance of the joint identified as 15° .

6. ACKNOWLEDGEMENTS

The authors are extremely thankful to Assoc. Prof. Dr. Semsettin TEMIZ and Prof. Dr. Erol SANCAKTAR for his valuable technical suggestions for improvement of the current paper. The work has been carried out with financial support by the Firat University Scientific Research Projects Management Unit (FÜBAP). (Project no: 1274)

7. REFERENCES

1. J. S. Tomblin, C. Yang and P. Harter, Investigation in thick bond line adhesive joint. Final Report, DOT/FAA/AR-01/33, US., Department of Transportation, Washington, DC., 2001.
2. L. P. Van Rijn, Towards the fastenerless composite design. *Composites Part .* **27A**, 915-920, 1996.
3. L. J. Hart-Smith, Adhesive-bonded single-lap joints, Nasa Report CR-112236, Langley Research Center, Hampton, VA., 1973.
4. K. Y. Lee and B. S. Kong, *J. Adhesion Sci. Technology*, **14**, 817-832, 2000.
5. T. Wah, Stress Distribution in a Bonded Anisotropic Lap Joint, Transactions of ASME, Series H, *J. of Engineering Materials and Technology*, **95**, 174-181, 1973.
6. D. J. Chang, and R. Muki, Stress Distribution in a Lap Joint under Tension-Shear, *Int. J. Solids Structures*, vol. **10**, 503-517, 1974.
7. P. Pfeiffer and M. Shakal, Effect of Bonded Metal Substrate Area and its Thickness on the Strength and Durability of Adhesively Bonded Joints, *Journal of Adhesion Science and Technology*, **12**, 339-348, 1998.
8. M. K. Apalak and R. Gunes, On non-linear thermal stresses in an adhesively bonded single-lap joint, *Computers and Structures*. **80**, 85-98, 2002.
9. A. Abedian and W. Szyszkowski, Effects of surface geometry of composites on thermal stress distribution a numerical study, *Composites Science and Technology*, **59**(1), 41-54, 1999.
10. E. Sancaktar and S. R. Simmons, Optimization of adhesively bonded single lap joints by adherend notching, *Journal of Adhesion Science and Technology*, **14**(11), 1363-1404, 2000.
11. A. F. Avila and P. O. Bueno, Stress analysis on a wavy-lap bonded joint for composites, *Int. Journal of Adhesion and Adhesives*, **24**, 407-414, 2004.
12. T. P. Lang and P. K. Mallick, Effect of spew geometry on stresses in single lap adhesive joints, *Int. J. Adhes*, **18**, 167-177, 1998.
13. A. Ozel, M. D. Aydin and Ş. Temiz, The effects of overlap length and adherend thickness on the strenght of adhesively bonded joints subjected to bending moment, *J. Adhesion Sci. Technology*, **18**(3), 313-325, 2004.
14. M. D. Aydin, A. Ozel and Ş. Temiz, The effect of adherend thickness on the failure of adhesively bonded single-lap joints, *J. Adhesion Sci. Technology*, **19**(8), 705-718, 2005.
15. M. Y. Solmaz, Mechanical analysis and design of adhesive bonded joints, *PhD Thesis*, Firat University, Elazig, 2008.
16. ANSYS, The general purpose finite element software, Swanson Analysis Systems, Houston, TX.
17. R. D. Adams and N. A. Peppiat, Stress Analysis of Adhesive Bonded Lap Joints, *J. of Strain Analysis*, **9**(3) 185-196, 1974.
18. M. D. Aydin, Experimental and theoretical investigation of mechanical properties of adhesive bonded single lap joint, *PhD. Thesis*, Ataturk University, Erzurum, 2003.
19. C. H. Wang and L. R. F. Rose, *J. Strain Anal*, **8**, 134. 1793.
20. R. D. Adams and J. A. Harris, *Int. J. Adhesion Adhesives* **17**, 17-25, 1997.